Journal for Educators, Teachers and Trainers
The PROFESIOLab electronic, peer-reviewed, open-access Magazine

ISSN 1989-9572

DOI: 10.47750/jett.2022.13.05.062

Characterization of Spin-Wave Eigenmodes in Normally Magnetized Nano-Pillars

1K.SURESH,
2Dr.KALAHASTI SIVADEVUNI

Journal for Educators, Teachers and Trainers, Vol.13 (5)
https://jett.labosfor.com/

Date of Reception: 12 July 2022

Date of Revision: 13 Aug 2022

Date of Acceptance: 20 September 2022

K.SURESH, Dr.KALAHASTI SIVADEVUNI (2022). Characterization of Spin-Wave Eigenmodes in Normally Magnetized Nano-Pillars. Journal for Educators, Teachers and Trainers, Vol.13(5). 658-672.

Journal for Educators, Teachers and Trainers
The LabOSfor electronic, peer-reviewed, open-access Magazine

Journal for Educators, Teachers and Trainers, Vol. 13(5)

ISSN1989 –9572
https://jett.labosfor.com

Characterization of Spin-Wave Eigenmodes in Normally Magnetized Nano-Pillars

1K.SURESH,2Dr.KALAHASTI SIVADEVUNI
12Assistant Professor
DEPT of H&S
Vaagdevi College of Engineering, Warangal, TS, India

Abstract The eigen-modes of spin waves in a circular spin-valve nano-pillar that is perpendicularly magnetised along z are studied spectroscopically and reported here. Magnetic Resonance Force Microscopy (MRFM) is used to conduct spectroscopy. Depending on whether an RF current running perpendicularly through the layers or a homogeneous in-plane RF magnetic field excites the nano-pillar, different spectra are observed. These findings are consistent with micromagnetic simulations of the local magnetization's time decay response to excitations with various azimuthal symmetries, (x iy)e−i4. Because of the orthoradial symmetry of the induced RF Oersted field, only four 0 modes are stimulated by the RF magnetic field and only four 1 modes are excited by the RF current, indicating that the azimuthal 4-index is the discriminating parameter for the selection criteria.

1.1 Introduction

A new science focused on harnessing spin dependent effects in the electrical transport characteristics has emerged as a result of technological advancements in the creation of hybrid nanostructures employing magnetic metals [1]. Two magnetic layers are separated by a normal layer in a basic spintronics device. It displays both the opposite spin transfer phenomenon [4, 5] and the well-known giant magneto-resistance (GMR) effect [2, 3].

From an experimental perspective, it is still necessary to precisely identify the

spin-wave (SW) eigen-modes in hybrid magnetic nanostructures [6–11]. The precise kind of modes induced by a polarised current in spin transfer nano-oscillators (STNOs) is of special interest. Finding the associated symmetry underlying each mode is crucial in this situation. It provides a basic understanding of their selection criteria and potential mutual connection processes.

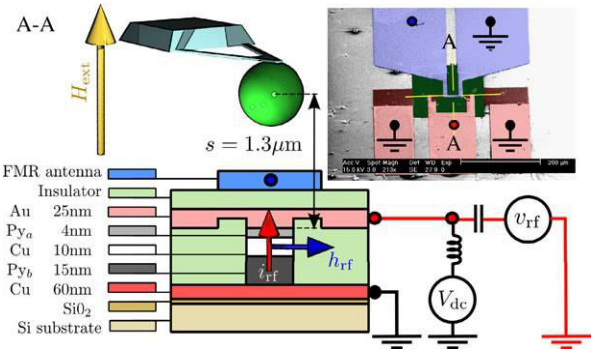

Fig. 1.1 Schematic representation of the experimental setup. Two independent excitation circuits are used: *in red*, the circuit allowing the injection of an RF current perpendicular-to-planethrough the nano-pillar (*i*rf, *redarrow*);*inblue*,thecircuit allowing the generation of an RF in-plane magnetic field (*h*rf, *blue arrow*) intraorinterSTNOs.Italsodeterminestheoptimumstrategytocoupletotheauto-oscillatingmodeobservedwhenthespintransfertorquecompensatesthedamping, a vital knowledge to achieve phase synchronization in arrays of nano-pillars [12]. TheseSWmodesalsohaveafundamentalinfluenceonthehighfrequencyproper-tiesofspin-valvedevices,andinparticularonthenoiseofmagneto-resistivesensors [13, 14].

This work concentrates on a comprehensive identification of the SW eigen-modes in a normally magnetized circular spin-valve nano-pillar, where the axial symmetry is preserved. We shall perform a comparative spectroscopic study ofthe SW modes excited either by an RF current flowing perpendicularly throughthe nano-pillar, as used in spin-torque driven ferromagnetic resonance (ST-FMR) [15,16],orbyahomogeneousRFin-planemagneticfield,asusedinconventional

FMR.Theexperimentalspectraarecomparedtomicromagneticsimulationsofthe time decay response of the local magnetization to a small perturbation of the mag- netic configuration. This allows identifying and labeling the observed SW eigen- modes, according to their symmetry and to the dipolar coupling between the two magnetic layers.

Thespin-valvestructureusedinthisstudyisastandardPermalloy ($Ni_{80}Fe_{20}$Py) bi-layer st±ucture sandwiching a 10 nm copper (Cu) spacer: the thicknesses of the thin $Py_a$and the thick Py_blayers are respectively t_a=4 nm and t_b=5nm.Theextendedfilmispatternedbystandarde-beamlithographyandion-milling techniques to a nano-pillar of radius 125 nm. The magnetic parameters of this sample have been measured in [17], and are reported in Table 1.1. The top Cu andbottomAucontactelectrodesareshowninredinFig.1.1.Theyareimpedance matched to allow for high frequency characterization by injecting an RF current i_{rf} through the device. Hereafter, spectra associated to SW excitations by this part of the microwave circuit will be displayed in a red tone.

The originality of our design is the addition of an independent top microwave antennawhosepurposeistoproduceanin-planeRFmagneticfieldh_{rf} atthenano- pillar location. In Fig. 1.1, this part of the microwave circuit is shown in blue. In- jecting a microwave current from a synthesizer inside the top antenna produces a homogeneousin-planelinearlypolarizedmicrowavemagneticfield,orientedperpendicularlytothestripedirection.Hereafter,spectraassociatedtoSWexcitations by this part of the microwave circuit will be displayed in a blue tone.

We shall use in this study a method independent of transport to detect the mag- neticresonanceinsideaspin-valvenanostructure:aMagneticResonanceForceMi- croscope(MRFM)[18–20],hereafternamedmechanical-FMR.Afirstdecisiveadvantageofthemechanical-FMRtechniqueisthatthedetectionschemedoesnotrelyontheSWspatialsymmetrybecauseitmeasuresthechangeinthelongitudinalcomponentofthemagnetization.Itthusprobes*all*theexcitedSWmodes,independentlyof their phase [21, 22]. A second decisive advantage is that mechanical-FMR is a verysensitivetechniquethatcanmeasurethemagnetizationdynamicsinnanostructuresburiedundermetallicelectrodes[23].Indeed,theprobeisamagneticparticle attachedattheendofasoftcantileverandiscoupledtothesamplethroughdipolar interaction.

Themechanicaldetectorconsistsofa800nmdiametersphereofsoftamorphous Fe (with 3 % Si) glued to the apex of an Olympus Bio-Lever having a spring

≈

con- stant k5 mN/m. In our setup, the separation between the center of the spherical probe and the nano-pillar is set to 1.3 µm (see Fig. 1.1), which is a large distance consideringthelateralsizeofthesample.Theexternalmagneticfieldproducedby an electromagnet is oriented out-of-plane, exactly along the nano-pillar axis z. In ourstudy,thestrengthoftheappliedmagneticfieldshallexceedthesaturationfield (8 kOe), so that the nano-pillar is studied in the saturated regime. The mechan- ical sensor measures then the spatial average of the longitudinal component $M_z$of magnetization:

$$\langle M_z \rangle \equiv \frac{1}{V}\int_V M(\boldsymbol{r}) d^3\boldsymbol{r}, \qquad (1.1)$$

1.2 IdentificationoftheSpin-WaveModes

In this section, we discuss the boundary-value problem for SW propagation inside normallymagnetizeddisks,where theconfinementleadsto adiscreteSWspectrum.

Neglecting the thickness dependence, only three indices are required to label the resonance peaks: the usual azimuthal and radial indices for a single disk (4,m), plus an additional index referring to the anti-binding or binding (A or B) coupling between the two magnetic layers in mutual dipolar interaction.

1.2.1 SingleMagneticDisk

SWeigen-modesarethesolutionsofthelinearizedequationofmotionofthemag- netization, obtained by decomposing the instantaneous magnetization vector $\boldsymbol{M}(t)$ into a static and dynamic component [25]:

$$\frac{\boldsymbol{M}(t)}{M_s} = \hat{\boldsymbol{u}} + \boldsymbol{m}(t) + O(\|\boldsymbol{m}\|^2), \qquad (1.2)$$

where the transverse component $\boldsymbol{m}(t)$ is the small dimensionless deviation ($\boldsymbol{m} \perp \hat{\boldsymbol{u}}$, $\|\boldsymbol{m}\| \ll 1$) ofthemagnetizationfromthelocalequilibriumdirection,$\boldsymbol{u}$.Inferromagnets, $|\boldsymbol{M}| = M_s$isaconstantofthemotion,sothatthelocalorthogonalitycondition $\hat{\boldsymbol{u}}\cdot\boldsymbol{m} = 0$is required.

We restrict our study to the case of thin layers so that one can assume that the magnetization dynamicsisuniformalongthethickness.Foranormallymagnetized

disk,where$\boldsymbol{uz}$,theSWmodescanbeclassifiedaccordingtotheirbehaviorunder rotations in the x–$y$plane (2D vector equations with polar coordinates $\rho$and ϕ):

$$\boldsymbol{m}_{4}=\frac{1}{\sqrt{2}}(\boldsymbol{x}\hat{}+i\boldsymbol{y}\hat{})e^{-i4\phi}\psi(\rho), \qquad (1.3)$$

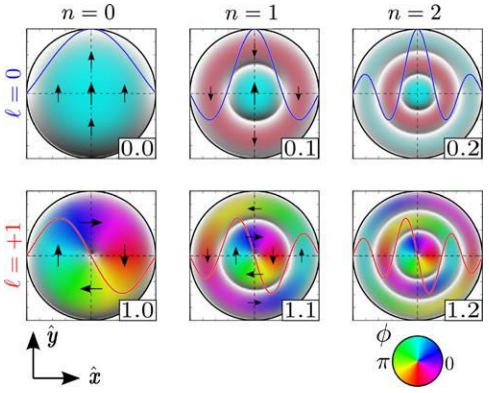

Fig.1.2 Colorrepresentation of the Bessel spatial patterns for different values of the azimuthal mode index *4* (*by row*)andradialmodeindex *n*(*bycolumn*).The*arrows*area snapshot of the transverse magnetization $\boldsymbol{m}_{v}$,labeledby theindex *v=4,n*

The top left panel shows the *v*0,0 (*4*0, *n*0) mode, also called the uni- form mode. It usually corresponds to the lowest energy mode since all the vectors are pointing in the same direction at all time. Below is the *4*1, *n*0 mode. It corresponds to SWs that are rotating around the disk in the same direction as the Larmorprecession.Thecorrespondingphaseisinquadraturebetweentwoorthog-onalpositionsandthismodehasanodeatthecenteroftheDisk.Thevariationupon the*n*0,1,2 index (*4* being fixed) shows higher order modes with an increasing

number of nodal rings. Each ring separates regions of opposite phase along the radial direction. All these spatial patterns preserve the rotation invariance symmetry.

The coupling to an external coherent source depends primarily on the 4-index [27] as the excitation efficiency is proportional to the overlap integral

$$h_v \propto (\boldsymbol{m}_v \cdot \boldsymbol{h}_1), \qquad (1.4)$$

where $\boldsymbol{h}_1(\boldsymbol{r})$ is the spatial profile of the external excitation field. It can be easily shown that a uniform RF magnetic field, $\boldsymbol{h}_1 = h_{rf}\boldsymbol{x}$, can only excite $4 = 0$ SW modes. Obviously, the largest overlap is obtained with the so-called uniform mode ($n = 0$). Higher radial index modes ($n \neq 0$) still couple to the uniform excitation but with a strength that decreases as n increases [19,28]. The $4 \neq 0$ normal modes, however, are hidden because they have strictly no overlap with the excitation. In contrast, the RF current-created Oerstedfield, $\boldsymbol{h}_1 = h_{Oe}(\rho)(-\sin\phi\boldsymbol{x} + \cos\phi\boldsymbol{y})$ has an orthoradial symmetry and can only excite $4 = \pm 1$ SW modes.

1.2.2 Double Magnetic Disks

The interaction between two identical magnetic layers leads to the splitting of the uniform mode in each layer into two collective modes: the binding and anti-binding modes. This has been observed in interlayer-exchange-coupled thin films [29] and in trilayered wires where the two magnetic stripes are dipolarly coupled [30]. In the case where the two magnetic layers are not identical (different geometry or mag- netic parameters), this general picture continues to subsist. Although both isolated layers have eigen-modes with different eigen-frequencies, the collective magnetiza- tion dynamics in each layer are still symmetrically or anti-symmetrically coupled. But here, the precession of magnetization can be more intense in one of the two layers and the spectral shift of the coupled SW modes with respect to the isolated SW modes is reduced, as it was observed in both the dipolarly-[30] and exchange-coupled cases [31].

Here, we assume that the dominant coupling mechanism between the two mag- netic disks in the nano-pillar is the dipolar interaction. We neglect any exchange coupling between the magnetic layers mediated through the normal spacer or any coupling associated to pure spin currents [7,32] in our all-metallic spin-valve struc- ture. Our nano-

pillarconsistsoftwodislikemagneticlayers,havingdifferentthick- nesses, with $t_a < t_b$, and different saturation magnetizations, with $M_a < M_b$. In the normally saturated state which is considered here, this difference of magnetization leads to a difference in the internal demagnetizing field of each layer (self dipolarcoupling)andinthestrayfieldofonelayerontheotherone(crossdipolarcoupli ng). Asaresult,theeigen-frequencyoftheuniformmodeofthethinlayerislargerthan the oneof the thicklayer, $\omega_a > \omega_b$. This is representedin Fig.1.3(a), onboth sides of the bi-layer diagram, where we have reported on an energy scale their relative positions.

In the perpendicular geometry, the strength of the dynamical dipolar couplingΩbetweenthelayersdependsonthecrosstensorelementjj'^{r},associatedtoth e in-plane component of the dipolar magnetic field produced inside layer j by thein-planecomponentof the magnetization of layer j'^{r}(see [17, 33]). It is attractive (lowerinenergy)whenbothlayersprecessinanti-phasebecausethedynamical
dipolar charges in each layer are alternate (anti-ferromagnetic coupling). Thus the binding state corresponds to a collective motion where the two layers vibrate anti- symmetrically (B) and the anti-binding state to a collective motion where they vi- brate symmetrically (A). In this case, the larger of the frequencies (ω_a) shifts upby

$$\Delta\omega = \frac{\Omega^2}{\omega_a - \omega_b}, \qquad (1.5)$$

while the smaller one (ω_b) shifts down by the same amount. This effect is summa- rized in Fig. 1.3.

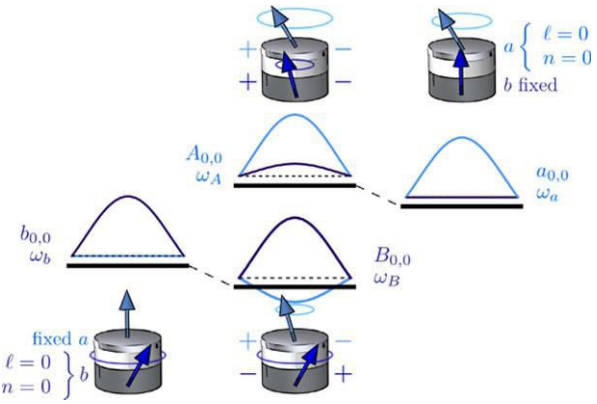

Fig.1.3 Schematicrepresentationofthecoupleddynamicsbetweentwodifferent magneticdisks. When the two disks are dynamically coupled through the dipolar interaction, the binding state *B*correspondstothetwolayersoscillatinginanti-phaseatω_B,withtheprecessionoccurringmostly inthethicklayer,whereastheanti-bindingstate*A* correspondstothelayersoscillatinginphaseat ω_A, with the precession mostly in the thin layer

amplitudesinthetwolayersisgivenby

$$|c_b/c_a|_{\omega A}=\Delta\omega/(\gamma h_{a,b})'_{\omega} \frac{\Omega}{\omega_a-\omega_b}. \quad (1.6)$$

Fortheexperimentalparameters,$\Omega/(\omega_a-\omega_b)\approx 0.1$,i.e.,theprecessionamplitude inthedisk*b* isabout10%ofthatinthedisk*a*.Thus,althoughthedipolarcoupling inducesasmallspectralshift(secondorderinthecouplingparameter(1.5)),itsin- fluenceintherelativeprecessionamplitudeissignificant(firstorderinthecouplin g parameter (1.6)).

1.2.3 MicromagneticSimulationsvs.Mechanical-FMR Experiments

Althoughtheanalyticalformalismpresentedaboveallowsestimatingthespectru m, several approximations have been made. In particular, we have assumed total pin- ning at the disks boundary for the SW modes and no variation of the precession profile along the disks thicknesses (2D model), and we have neglected the depen- dence on the mode index *v*of the dynamicdipolarcoupling.Instead of developing a more complex analytical

formalism, we have performed a complete calculation of the SW spectra inside our nano-pillar sample using the open source micromag- netic simulation package Nmag [34]. Nmag is a finite element solver based on the generalpurposemulti-physicslibraryNsim.ItisdevelopedbythegroupofH.Fan-gohrandT.FischbacherintheSchoolofEngineeringSciencesattheUniversityof Southampton.

Table 1.1 Magnetic parameters of the thin Py*a*and thick Py*b*layers measured by mechanical- FMR in the nano-pillar

$4\pi M_a$(G)	α_a	$4\pi M_b$(G)	α_b	γ(rads—1_G—$1_)$
8.0×10^3	1.4×10^{-2}	9.6×10^3	0.85×10^{-2}	1.87×10^7

Inthissimulation,thefullthree-dimensional(3D)dynamicsofthebi-layersystem is calculated. The thin layer is discretized with a mesh of 4 nm (equal to its thickness), and the thick layer with a mesh of 3 nm. The numbers of nodes are respectively6135inthethinlayerand37598inthethicklayer.Themagneticparameters introduced in the code are the ones reported in Table 1.1. The magnetization vectorisassumedtobeuniforminsideeachcell,whichisvalidbecausethecellsize issmallerthantheexchangelength Λ5nm inPermalloy.Weemphasizethatthe simulationsincorporatetheperturbingpresenceofthemagneticsphereattached on theMRFMcantilever.Moreover,the10nmthickCuspacerisreplacedbyvacuum , so that the layers are only coupled trough the dipolar interaction (spin diffusion effects are absent).

The first step is to calculate the equilibrium configuration of the normally mag- netizednano-pillaratH_{fix}10 kOe.The externalmagneticfieldis appliedexactly = × along z and the spherical probe with a magnetic moment $m210^{-10}$ emu is placedontheaxialsymmetryaxisatadistance$s$1.3μmabovetheuppersurface of the nano-pillar (see Fig. 1.1). The convergence criterion introduced in the code is $1/M_s dM/dt<1°$/ns. The result reveals that the equilibrium configuration is almost uniformly saturated along z. Still, a small radial flaring (<5°) of the mag- netization from z is observed at the periphery of the thick and thin layers.

InordertocalculatetheSWspectrumcorrespondingtoagivenexcitationofthis equilibrium state at H_{fix}10 kOe, we record the time decay response of the local magnetizationtoasmallperturbationofthemagneticconfiguration,andweFourier transform the ringdown of the transverse magnetization [35]. Two different initial conditions are simulated. For the conventionalFMR spectrum, in which a uniform RFfieldisusedtoexciteSWmodes,weusethefollowingperturbationvectorfield:

$$\boldsymbol{m}=\vartheta \quad J_0(k_{0n}\rho)\hat{\boldsymbol{x}}. \qquad (1.7)$$
$$n<6$$

Thisformcorrespondstoanexcitation whichputsthesameenergyinthelowest 6

=

n-index modes with azimuthal index *4*0. For the spectrum excited by an RF current flowing through the nano-pillar, which creates an orthoradial RF Oersted field in the magnetic volume, we use:

$$\boldsymbol{m}=\vartheta \quad J_1(k_{1n}\rho)(-\sin\phi\hat{\boldsymbol{x}}+\cos\phi\hat{\boldsymbol{y}}). \qquad (1.8)$$
$$n<6$$

Attime*t*0,weaddateverymeshtheperturbationvectorfielddefinedin(1.7) orin(1.8)totheelocalunitvectoralongtheequilibriummagnetization.Thefirstone

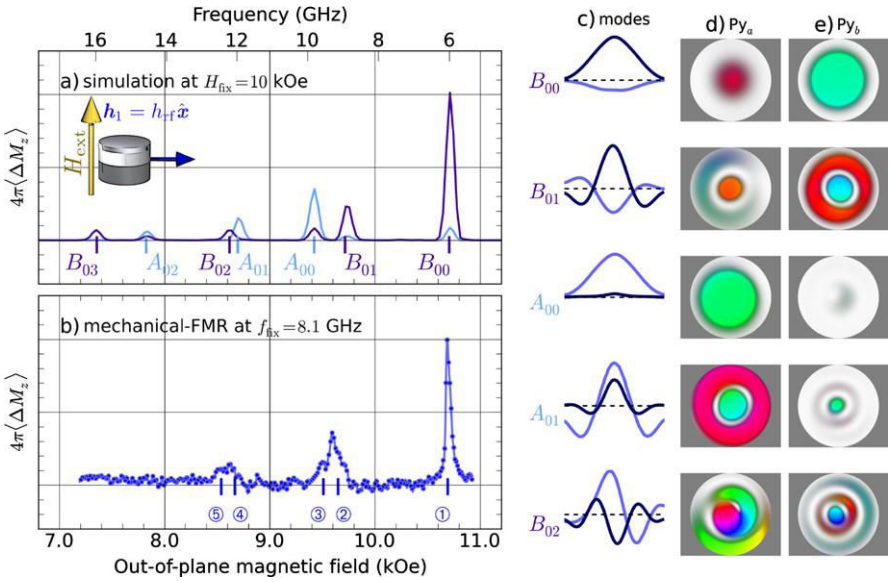

Fig.1.4 Panel(**a**)isthenumericallycalculatedspectralresponsetoauniformexcitation field $\boldsymbol{h}_1\boldsymbol{x}$, from a 3D micromagnetic simulation performed at H_{fix}10 kOe. The peaks are labeled according to their precession profiles shown in (**c**), (**d**), and (**e**). A *light* (*dark*) *color* is used to indicate the energy stored in the thin (thick) layer. Panel (**b**) shows the experimental spectrum measuredbymechanical-FMRwhenexcitingthenano-pillarbyahomogeneousRFmagneticfield at f_{fix}= 8.1 GHz

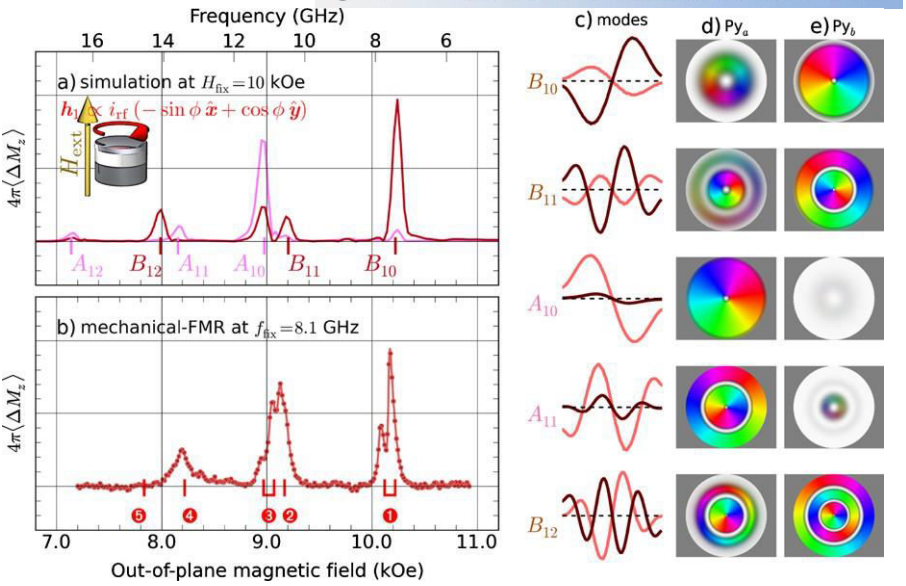

Fig.1.5 Panel(**a**)isthesimulatedspectralresponsetoanorthoradialexcitationfiel d $\propto -\hat{+}\hat{}$ $\boldsymbol{h}_1\sin\phi\boldsymbol{x}\cos\phi\boldsymbol{y}$.Panel(**b**)istheexperimentalspectrummeasuredbymechanical-FMRfor anRFcurrent excitation.Panels (**c**)–(**e**)showthesimulated precession patternsoftheeigen-vectors

1.3 Conclusion

In conclusion, we investigated the SW eigen-modes in the prototype of a STNO, a normally magnetisednano-pillar made of two magnetic layers in dipolar contact, using the MRFM method [20]. The SW spectra of this passive STNO stimulated by an RF current flowing perpendicularly across the layers and by a homogeneous in-plane RF magnetic field were compared. We discovered that the two aforementioned excitation techniques ignite rather distinct SW modes, each with an azimuthal index of 4 0 and 4 1, respectively. Additionally, we created a straightforward analytical theory that offers a thorough labelling of every SW eigen-mode of a magnetic nano-pillar in the axially symmetric scenario under study. The standard azimuthal and radial indices 4 and n, which are used for the SW modes of a single magnetic disc, as well as an extra index that refers to the binding or anti-binding (B or A) dipolar coupling between the two magnetic discs are needed for this labelling. The outcomes of 3D micromagnetic simulations using the Nmag software were also contrasted with the experimental and analytical findings that were achieved. We discovered that the discriminating parameter for the selection rules of the SW mode excitation is the 4-index, which is associated with the azimuthal symmetry of the SW modes. Our findings, in our opinion, are

crucial for both the experimental determination of the STNO parameters and the optimisation of the properties of nano-spintronic devices, and specifically STNOs.

References

1. S.Wolf,D.D.Awschalom,R.A.Buhrman,J.Daughton,S.vonMolnar,M.L.Roukes, A.Y.Chtchelkanova,D.M.Treger,Science**294**,1488(2001)
2. M.N.Baibich,J.M.Broto,A.Fert,F.N.V.Dau,F.Petroff,P.Etienne,G.Creuzet, A.Friederich, J.Chazelas,Phys.Rev.Lett.**61**(21),2472(1988)
3. G.Binasch,P.Grunberg,F.Saurenbach,W.Zinn, Phys.Rev.B**39**(7),4828 (1989)
4. J.Slonczewski,J.Magn.Magn.Mater.**159**,L1(1996).doi:10.1016/0304-8853(96)00062-5
5. L.Berger,Phys.Rev.B**54**(13),9353(1996)
6. V.E. Demidov, S.O. Demokritov, B. Hillebrands, M. Laufenberg, P.P. Freitas, Appl. Phys. Lett. **85**(14), 2866 (2004). doi:10.1063/1.1803621
7. G.Woltersdorf,O.Mosendz,B.Heinrich,C.H.Back,Phys.Rev.Lett.**99**(24), 246603(2007). doi:10.1103/PhysRevLett.99.246603
8. G.deLoubens,V.V.Naletov,O.Klein,J.BenYoussef,F.Boust,N.Vukadinovic,Phys.Rev. Lett. **98**(12), 127601 (2007)
9. G.deLoubens,V.V.Naletov,M.Viret,O.Klein,H.Hurdequint,J.BenYoussef,F.Boust, N.Vukadinovic,J.Appl.Phys.**101**,09F514(2007)
10. G.Gubbiotti,M.Madami,S.Tacchi,G.Carlotti,H.Tanigawa,T.Ono,J.Phys.D, Appl.Phys. **41**(13),134023(2008).doi:10.1088/0022-3727/41/13/134023
11. P.S.Keatley,V.V.Kruglyak,A.Neudert,E.A.Galaktionov,R.J.Hicken,J.R.Childress, J.A.Katine,Phys.Rev.B**78**(21),214412(2008).doi:10.1103/PhysRevB.78.214412